ELSEVIER

Biochimica et Biophysica Acta 1553 (2002) 320–330

BIOCHIMICA ET BIOPHYSICA ACTA
BBA

www.bba-direct.com

# Rapid-scan Fourier transform infrared spectroscopy shows coupling of GLu-L212 protonation and electron transfer to $Q_B$ in *Rhodobacter sphaeroides* reaction centers

Alberto Mezzetti [a,b], Eliane Nabedryk [a], Jacques Breton [a], Melvin Y. Okamura [c], Mark L. Paddock [c], Giovanni Giacometti [b], Winfried Leibl [a,*]

[a] *Section de Bioénergétique, CEA Saclay, Bât 532, 91191 Gif-sur-Yvette, France*
[b] *Department of Physical Chemistry 'A. Miolati', Via Loredan 2, 1-35100 Padova, Italy*
[c] *Department of Physics, University of California, San Diego, 9500 Gilman Drive, La Jolla, CA 92093, USA*

Received 24 August 2001; received in revised form 4 December 2001; accepted 10 January 2002

**Abstract**

Rapid-scan Fourier transform infrared (FTIR) difference spectroscopy was used to investigate the electron transfer reaction $Q_A^- Q_B \rightarrow Q_A Q_B^-$ ($k_{AB}^{(1)}$) in mutant reaction centers of *Rhodobacter sphaeroides*, where Asp-L210 and/or Asp-M17 have been replaced with Asn. Mutation of both residues decreases drastically $k_{AB}^{(1)}$, attributed to slow proton transfer to Glu-L212, which becomes rate limiting for electron transfer to $Q_B$ [M.L. Paddock et al., Biochemistry 40 (2001) 6893]. In the double mutant, the FTIR difference spectrum recorded during the time window 4–29 ms following a flash showed peaks at 1670 (−), 1601 (−) and 1467 (+) $cm^{-1}$, characteristic of $Q_A$ reduction. The time evolution of the spectra shows reoxidation of $Q_A^-$ and concomitant reduction of $Q_B$ with a kinetics of about 40 ms. In native reaction centers and in both single mutants, formation of $Q_B^-$ occurs much faster than in the double mutant. Within the time resolution of the technique, protonation of Glu-L212, as characterized by an absorption increase at 1728 $cm^{-1}$ [E. Nabedryk et al., Biochemistry 34 (1995) 14722], was found to proceed with the same kinetics as reduction of $Q_B$ in all samples. These rapid-scan FTIR results support the model of proton uptake being rate limiting for the first electron transfer from $Q_A^-$ to $Q_B$ and the identification of Glu-L212 as the main proton acceptor in the state $Q_A Q_B^-$. 

*Keywords:* Proton uptake; Bacterial photosynthesis; Proton-coupled electron transfer; Site-directed mutation; *Rhodobacter sphaeroides*

## 1. Introduction

Photosynthetic reaction centers (RCs) of purple bacteria are integral membrane enzymes, which function as light-driven quinone reductases. Absorption of a photon leads to ultrafast charge separation between the primary electron donor P, a special pair of BChl, and the primary electron acceptor $Q_A$, a quinone molecule. A second quinone, $Q_B$, accepts successively two electrons from $Q_A$ and two protons from the cytoplasm through a pathway formed by amino acid side chains and water molecules. The

Abbreviations: FTIR, Fourier transform infrared; RC, reaction center; $Q_A$, $Q_B$, primary, secondary quinone acceptor; DAD, 3,6 diaminodurene(2,3,5,6-tetramethyl-*p*-phenylenediamine); Tris, Tris(hydroxymethyl)aminomethane

* Corresponding author. Fax: +33-1-6908-8717.
*E-mail address:* leibl@dsvidf.cea.fr (W. Leibl).

0005-2728/02/$ – see front matter 
PII: S0005-2728(02)00186-X

quinol thus formed is released from the $Q_B$ binding site and replaced by an oxidized quinone from the pool of quinones in the lipid membrane (see [1] for a review). Whereas quinones are ubiquitous electron carriers in bioenergetic systems, photosynthetic RCs offer the advantage to synchronize the reaction sequence by short light flashes. This makes them ideal model systems to investigate general principles governing the kinetics and energetics of quinone redox chemistry in proteins.

The structure of the RC of *Rhodobacter sphaeroides* has been solved by X-ray crystallography to high resolution [2–4]. This led to a detailed knowledge of the position of pigments, cofactors and amino acids, and of their relative distance and orientation. With this structural information, it became possible to give a much deeper interpretation of spectroscopic data in order to understand the molecular mechanisms underlying the function of these enzymes. In addition, for *Rb. sphaeroides*, site-directed mutagenesis is well established, which allows changing of specific amino acids. Mutant RCs provide an excellent tool to investigate the role of the protein in electron and/or proton transfer processes and functional studies on such mutant RCs contributed much to the present knowledge about which amino acids are essential for the function of the quinone acceptor complex [1,5,6].

It is generally accepted that in isolated RCs the first electron transfer from $Q_A^-$ to $Q_B$ does not involve direct protonation of $Q_B$, which occurs only on the second reduction step. However, formation of the semiquinone $Q_B^-$ (and to a lesser extent of $Q_A^-$) is accompanied by a sub-stoichiometric proton uptake by the protein. Various observations on mutant RCs [1,7–9] and electrostatic calculations [10,11] on native RCs suggested that the protonation of the side chains of the amino acids Glu-L212 and/or (depending on pH) Asp-L213, located close to $Q_B$ ($\sim$5 Å), is responsible for this proton uptake. A complication arises from the fact that these residues are part of a cluster of strongly interacting carboxylic residues, making it difficult to attribute individual p$K_a$ values to specific protonatable groups. Rather the non-stoichiometric proton uptake is likely to lead to increased protonation distributed over several groups whereby the involved groups may vary as a function of the pH in the bulk.

Recently the pathway for protons from the cytoplasmic surface towards the cluster of carboxylic acids close to $Q_B$ has been established (Fig. 1). It involves the side chain of two aspartic acids, namely Asp-L210 and Asp-M17 [12,13]. Optical measurements have shown that the mutation of both these amino acids to Asn leads to a strong, $\sim$60-fold decrease of $k_{AB}^{(1)}$, the rate of the first electron transfer to $Q_B$, as well as of proton uptake [13]. This surprising result (in view of the fact that $Q_B$ is not protonated upon first reduction) was explained by a model in which the proton transfer into the cluster of carboxylic residues close to $Q_B$ acts as a rate-limiting step for the first electron transfer to $Q_B$ [1,13]. In fact, the pioneering work of Graige and coworkers [14] measuring the rate constant $k_{AB}^{(1)}$ as a function of driving force had clearly demonstrated that electron transfer is not the rate-limiting step for the first reduction of $Q_B$. Identification of the rate-limiting step, however, remained elusive and different mechanisms including conformational changes, possibly implying movement of the quinone from a distal to a proximal binding position, had been evoked [14,15].

To study the molecular mechanisms governing the function of $Q_B$, one of the most promising spectroscopic techniques is FTIR difference spectroscopy as

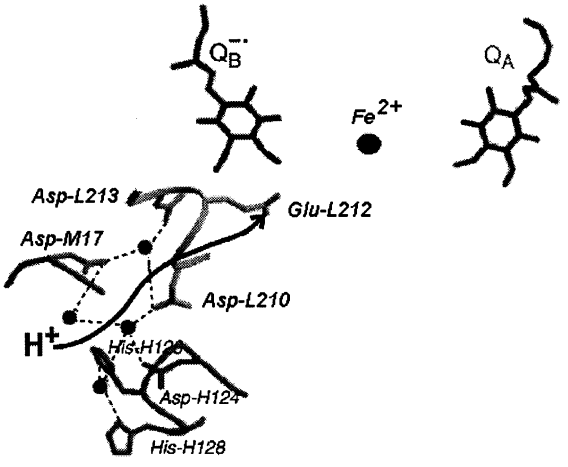


Fig. 1. Pathway (arrow) for proton transfer from the cytoplasmic surface to Glu-L212 in concomitance with $Q_B$ reduction. Note the location of both Asp-L210 and Asp-M17 about halfway between $Q_B$ and the proton entry point. Circles represent water molecules. Also shown are $Q_A$, the electron donor to $Q_B$, as well as the non-heme iron between $Q_A$ and $Q_B$. Modified from [29] based on the light-adapted RC structure [15] (Protein Data Bank entry 1AIJ).

it permits to monitor reaction-induced changes in vibrational modes of both the protein and the cofactors simultaneously. A large amount of data has been obtained on RCs of *Rb. sphaeroides* by static FTIR difference spectroscopy [16–18]. These studies have led to the precise identification of IR marker bands for specific redox states of cofactors, in particular the primary donor and the two quinone acceptors [16,18]. In the last 15 years, time-resolved FTIR spectroscopy has been increasingly applied to the study of enzymatic reactions that can be triggered by light [19–22]. Compared to static FTIR difference spectroscopy, time-resolved FTIR difference spectroscopy can monitor the evolution of a reaction, revealing the concomitance or the non-concomitance of different molecular events, e.g., the reduction of a cofactor and the concomitant protonation of a nearby amino acid residue. Two different techniques are mainly used, rapid-scan FTIR [19] and step-scan FTIR spectroscopy [23]. The step-scan technique can be applied to the study of quickly reversible reactions and allows for a time resolution of $\sim$30 ns. The rapid-scan technique is much more limited in time resolution, the latter being essentially given by the maximal speed of the moving mirror (millisecond time domain). On the other hand, this technique is much more straightforward and can be easily applied to not quickly reversible systems. Several IR and FTIR kinetic techniques have been previously applied to the study of photoreduction of quinones in bacterial RCs of *Rb. sphaeroides*. Light-induced intermediates in native RCs were first investigated by rapid-scan FTIR difference spectroscopy allowing for the first time the only contributions of $Q_A$, $Q_A^-$, $Q_B$, and $Q_B^-$ to be revealed [24]. In native RCs from *Rb. sphaeroides* the first electron transfer from $Q_A^-$ to $Q_B$ proceeds with a kinetics of $\sim$200 μs at room temperature [25] and therefore is not accessible to the rapid-scan technique. Transient signals associated with $Q_A^-Q_B \rightarrow Q_AQ_B^-$ electron transfer with 120–150 μs and ms half-times could be observed and characterized using tunable IR diode laser sources [26,27] or step-scan FTIR spectroscopy [28].

However, in specific mutant RCs, where the first electron transfer reaction is slowed down to the millisecond time domain, a rapid-scan FTIR investigation becomes possible. In this work we have applied the rapid-scan technique to study on a molecular level the reaction path connected with the first electron transfer from $Q_A^-$ to $Q_B$ in native RCs of *Rb. sphaeroides* and in the Asp-L210 → Asn/Asp-M17 → Asn [DN(L210)/DN(M17)], Asp-M17 → Asn [DN(M17)], and Asp-L210 → Asn [DN(L210)] mutant RCs. The results show that, within the temporal resolution, the time evolution of IR marker bands is the same for oxidation of $Q_A^-$, reduction of $Q_B$, and protonation of Glu-L212 in all samples. These findings confirm the model derived from visible spectroscopy that electron transfer and protonation of the carboxylic side chain of Glu-L212 are kinetically coupled [29]. A preliminary account of this work has been presented [30].

## 2. Materials and methods

### 2.1. Samples

The site-directed mutations Asp-L210 → Asn and Asp-M17 → Asn were constructed as described previously [31]. The double mutation of Asp-L210 → Asn/Asp-M17 → Asn was constructed in two sequential steps using the QuikChange Mutagenesis kit (Stratagene) and a Perkin Elmer PCR System [13].

RCs from *Rb. sphaeroides* R26 and the mutants strains were isolated in 15 mM Tris–HCl (pH 8), 0.025% lauryl dimethylamide-*N*-oxide (LDAO), as described in [32]. The samples for FTIR measurements were prepared as thin paste squeezed between two $CaF_2$ windows to yield an absorbance in the amide I region of the spectrum of 0.6–0.9 A.U. To guarantee full occupancy of the $Q_B$ site, an $\sim$10-fold excess of $UQ_6$ (Sigma) was added to the RC suspension. Ten mM Na-ascorbate and 20 mM 2,3,5,6-tetramethyl-*p*-phenylenediamine (DAD) were present as external redox components to ensure fast reduction of $P^+$. Complete reduction of $P^+$ is necessary as the amplitude of the $P^+/P$ difference spectrum is much larger (by about a factor of 5 [18]) than the amplitude of the difference spectra associated with quinone reduction and protonation of amino acid side chains. Thus even a minor contribution from $P^+/P$ would hamper kinetic analysis of the $Q_A^-Q_B \rightarrow Q_AQ_B^-$ reaction. To avoid contamination even of the first scan after the flash by $P^+/P$ contributions, a delay time of some milliseconds was inserted between the flash and

recording of the first interferogram. It is worth noting that in the case of mutant RCs, where electron transfer from $Q_A^-$ to $Q_B$ is slowed down to the tens of ms time range, this results in reduction of $P^+$ preceding the electron transfer between the quinones.

### 2.2. FTIR measurements

Rapid-scan experiments were performed following the method described in [19]. A Bruker IFS88 FTIR spectrometer equipped with a photoconductive MCT-A detector and with OPUS software was used. All measurements were made at 281 ± 1 K using a temperature-controlled $N_2$ cryostat. The photoreaction was triggered by a saturating flash from a frequency-doubled Nd:YAG laser (7 ns, ~20 mJ, Quantel, France). The velocity of the moving mirror was set to its maximal value (5.063 cm $s^{-1}$). Single-sided interferograms were acquired only during the forward movement of the mirror. With an optical filter (Lot-Oriel) the spectral range was limited to 2250–800 $cm^{-1}$. The spectral resolution was set to 4 $cm^{-1}$. The number of sampling points for each interferogram was 1141, 126 of which were taken before the centerburst (maximum intensity of the interferogram) for phase correction. With these instrumental conditions recording of an interferogram required 25 ms ('Take data' or TKDA period) and 48 ms were necessary to allow the mirror to complete its movement and to get back to the original position to start the next TKDA acquisition. Thus, interferograms were taken every 73 ms.

Experiments started with the recording of 40 interferograms, averaged to give a single 'background' interferogram. Then a laser flash was fired to trigger the reaction and after a delay time of 4 ms to allow external donors to completely reduce $P^+$ (see above) successive interferograms were recorded during up to 5 s. At delays longer than 700 ms five scans were averaged to give a single interferogram. The results from 2000 to 3000 cycles (obtained on two or three different samples) were averaged to improve the signal-to-noise ratio. Between cycles a delay time ranging from 2 to 3 min allowed a complete relaxation of the system (due to reoxidation of $Q_B^-$ by the external redox chemicals). At the end of the data acquisition, the stored interferograms were Fourier transformed to give the corresponding single beam spectra using the OPUS software and applying the Mertz phase correction mode and the Blackman–Harris 3-term apodization function. Difference spectra at various times after the laser flash were calculated according to the formula $\Delta A(t) = -\log [S(t)/S(0)]$, where $S(0)$ is the single beam spectrum obtained from the averaged interferogram recorded before the laser flash and $S(t)$ is the single beam spectrum recorded at time $t$. To exclude possible perturbations of the spectra due to the evolution of the reaction during recording of the interferograms a simulation analysis was carried out following the approach of Lephardt et al. [33] and that of Braiman et al. [19]. The analysis consisted in multiplying a difference interferogram corresponding to the pure reaction state with an increasing or decreasing exponential function. Fourier transformation and comparison of the spectra showed that spectral perturbations were negligible.

Static FTIR difference spectra were recorded on a Nicolet 60SX spectrometer as described [8,34]. Pure $Q_A^-/Q_A$ difference spectra were obtained using stigmatellin as inhibitor of electron transfer from $Q_A^-$ to $Q_B$ [35].

## 3. Results

### 3.1. Native RCs

Rapid-scan FTIR difference spectra induced by one laser flash in the native RCs are shown in Fig. 2. The spectra shown are the difference between the background spectrum taken before the laser flash and consecutive spectra recorded at various times after the laser flash. Therefore they represent the changes between the ground state and the charge-separated states which evolve in time with negative bands corresponding to the (disappearing) ground state vibrations and positive bands corresponding to (appearing) product state vibrations. The first scan recorded during the time window from 4 to 29 ms already yields a difference spectrum characteristic of the $Q_AQ_B \rightarrow Q_AQ_B^-$ transition as can be seen in particular by the marker bands at 1728 (+), 1640 (−), and 1479 (+) $cm^{-1}$ [8,36–38]. The band at 1640 $cm^{-1}$ is in part attributed to the C=O mode of $Q_B$ and the 1479 $cm^{-1}$ band is due to the $C–O^-$ stretching mode of the semiquinone $Q_B^-$. The 1728

$cm^{-1}$ band arises from the protonated side chain of Glu-L212 [8]. The state $Q_B^-$ is stable on a seconds time scale and the $Q_B^-/Q_B$ rapid-scan spectra compare well with the steady-state spectrum (Fig. 2, lowest trace, from [34]). Reduction of $Q_B$ faster than the time resolution of the rapid-scan technique is consistent with electron transfer from $Q_A^-$ to $Q_B$ in ~150 μs [25,26] and with protonation of Glu-L212 in ~1 ms as determined by single wavelength IR spectroscopy [27].

### 3.2. DN(L210)/DN(M17) double mutant

In the DN(L210)/DN(M17) double mutant the first scan recorded during the time window from 4 to 29 ms yielded a difference spectrum characteristic of the $Q_AQ_B \rightarrow Q_A^-Q_B$ transition (Fig. 3A) as can be seen in particular by the marker bands previously observed in native RCs at 1670 (−), 1601 (−), and 1467 (+) $cm^{-1}$ [16,24,35,39,40]. The band at 1670 $cm^{-1}$ is attributed to a protein mode [24], while the 1601 $cm^{-1}$ band has been proposed to arise from a

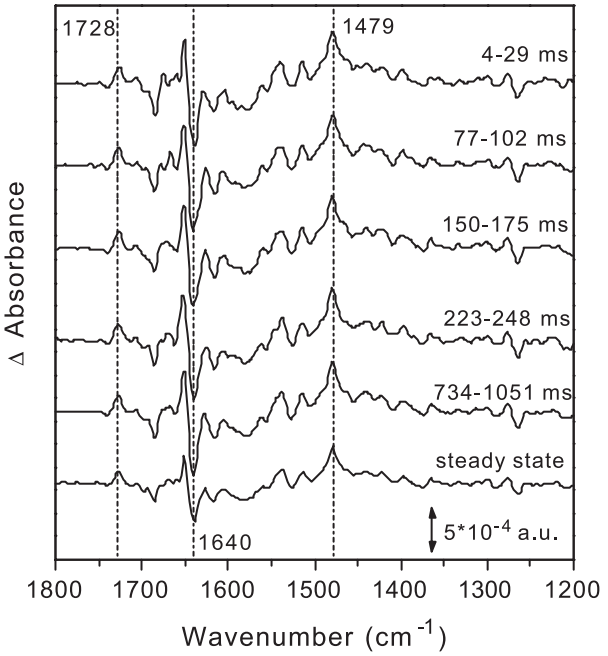


Fig. 2. Rapid-scan spectra of wild-type RCs at different times after a saturating laser flash. The times indicated are the TKDA period during which each interferogram is taken. The lowest trace represents the $Q_B^-/Q_B$ difference spectrum obtained under steady-state conditions (from [34]). Note the absence of temporal evolution in the spectra indicating fast formation of $Q_B^-$.

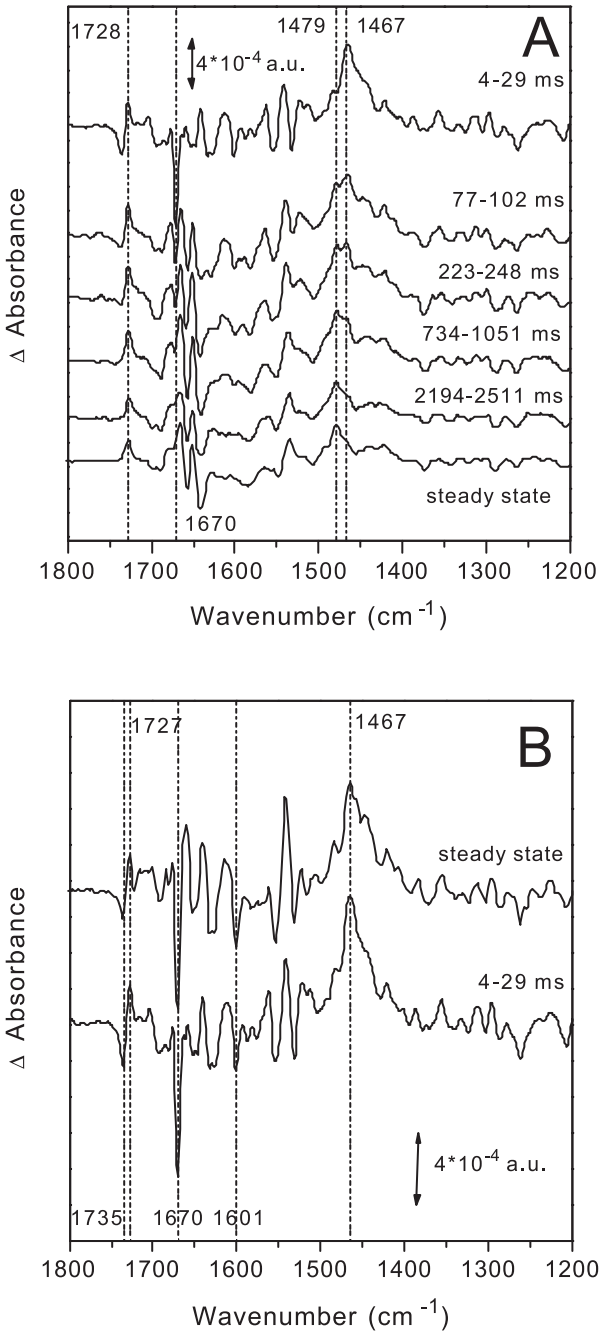


Fig. 3. (A) Rapid-scan spectra of the DN(L210)/DN(M17) double mutant at different times after a saturating laser flash. The times indicated are the TKDA period during which each interferogram is taken. The lowest trace represents the $Q_B^-/Q_B$ difference spectrum obtained under steady-state conditions (from [34]). (B) $Q_A^-/Q_A$ difference spectra in the DN(L210)/DN(M17) double mutant obtained under steady-state conditions in the presence of stigmatellin (upper trace) or by the first scan of the rapid-scan experiment (lower trace). Note the similarity between the two traces showing that $Q_A^-$ is present in the double mutant at short times.

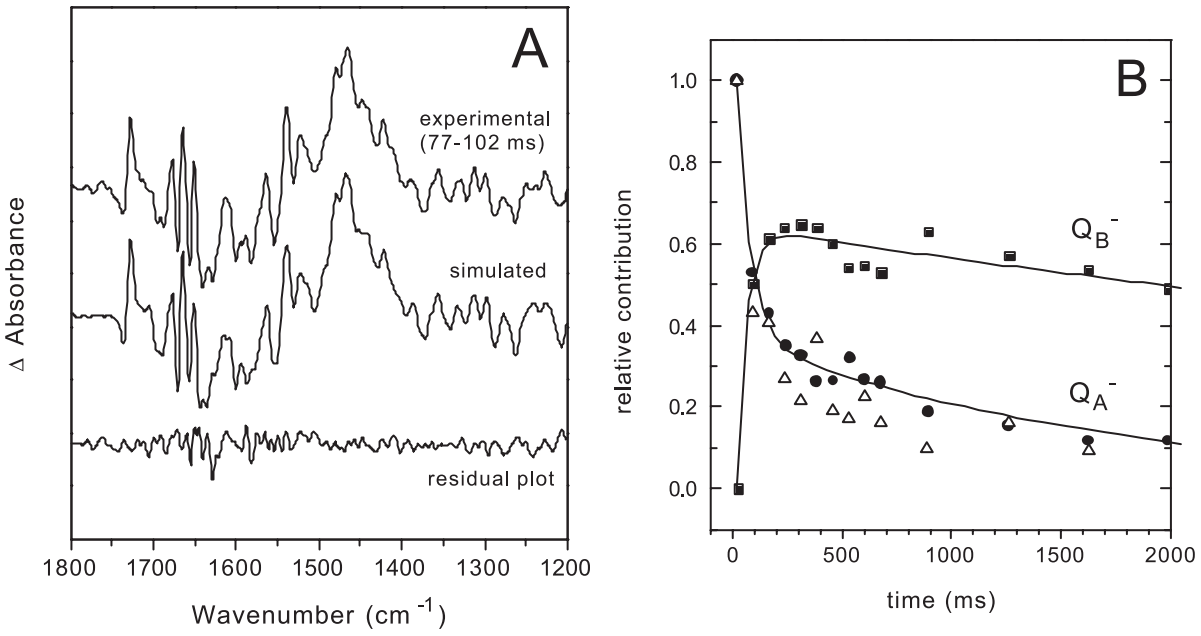


Fig. 4. Kinetic analysis of the evolution of the rapid-scan spectra in the DN(L210)/DN(M17) double mutant. (A) Comparison of the experimental difference spectrum recorded between 77–102 ms after the flash (upper trace) and the best fit of this spectrum as combination of pure $Q_A^-/Q_A$ (53%) and $Q_B^-/Q_B$ (47%) difference spectra (middle trace). The spectrum recorded between 4 and 29 ms was taken as reference for $Q_A^-/Q_A$ (see text and Fig. 3B) and a spectrum recorded in the static mode was taken as reference for $Q_B^-/Q_B$. The lowest trace shows the difference between the upper two traces. (B) Plot of the fractional contribution of $Q_A^-/Q_A$ (●) and $Q_B^-/Q_B$ (■) difference spectra as obtained by the global fit analysis of the rapid-scan spectra. Triangles (△) represent the amplitude of the band at 1670 $cm^{-1}$, characteristic of the $Q_A^-/Q_A$ difference spectrum. Solid lines represent best fits with two exponential kinetic phases with time constants of 40 ms (75%) and ~1 s (25%). See text for further details.

mode of mixed C=O and C=C character of $Q_A$ [16,39,40]. The 1467 $cm^{-1}$ band is due to the C–$O^-$ stretching mode of the semiquinone $Q_A^-$. This spectrum is essentially identical to a spectrum obtained for the same mutant in presence of the $Q_B$ inhibitor stigmatellin with static FTIR difference spectroscopy (Fig. 3B).

The second and following scans show evolution to the $Q_AQ_B^-$ state with bands at 1640 (−) and 1479 (+) $cm^{-1}$, which had been assigned to vibrational modes of $Q_B$ and $Q_B^-$, respectively [16,37,38], and at 1728 $cm^{-1}$ assigned to protonation of Glu-L212 [8,27,34]. Spectra taken at times longer than about 2 s are virtually indistinguishable from a spectrum taken under steady-state conditions (Fig. 3A, lowest trace, from [34]). A kinetic analysis of the time evolution of the marker bands at 1670 ($Q_A$) and 1479 $cm^{-1}$ ($Q_B^-$) yielded good fits with an exponential time constant of about 40 ms for the dominant phase. In addition a minor slow phase with a kinetics in the seconds range is observed for the band at 1670 $cm^{-1}$, which indicates slower reoxidation of $Q_A^-$ in about 25% of the RCs. The simplest explanation is that this represents a fraction of RCs without functional $Q_B$.

This kinetic analysis of single marker bands is straightforward only in cases where the band is large and clearly separated, like in the case of the negative band at 1670 $cm^{-1}$, characteristic for the $Q_AQ_B$ to $Q_A^-Q_B$ transition. In other cases such an analysis is complicated by the fact that at the given wavenumber absorption changes from different states overlap. An example (see Fig. 3A) is the positive band at 1728 $cm^{-1}$, which grows in with formation of $Q_B^-$ replacing a differential signal at 1735 (−) and 1727 $cm^{-1}$ (+), the latter decaying together with $Q_A^-$. This differential signal was attributed to an electrostatic effect on the vibrational mode of the 10a-ester C=O of the bacteriopheophytin $H_A$ due to the presence of the negative charge on the quinone $Q_A$ [41]. A more precise analysis of the rapid-scan kinetics that takes into account the information content of the whole spectral range requires global analysis of the spectra.

We have chosen to analyze the spectrum at a given time as combinations of pure $Q_A/Q_A^-$ and $Q_B/Q_B^-$ spectra. An example of such an analysis is shown in Fig. 4A for the rapid-scan spectrum recorded between 77–102 ms after the flash, where both difference spectra show comparable contributions. The fractional contributions of the $Q_A^-/Q_A$ and $Q_B^-/Q_B$ spectral features are plotted as a function of time of recording of the corresponding spectrum in Fig. 4B. The results of the analysis at a single wavelength (1670 $cm^{-1}$) are also shown (Fig. 4B, open triangles). It can be seen that the global analysis resulted in very similar kinetics as the analysis of discrete bands. $Q_A^-$ decays and $Q_B^-$ raises with a common kinetics of $\sim$40 ms. Decay of $Q_B^-$ in the seconds time range and of a minor fraction of $Q_A^-$ reflect reoxidation of the two semiquinones by an external electron acceptor ($DAD^+$). In addition, the investigation of the residual plots of the global analysis showed that no intermediate state is detectable (Fig. 4A). In summary, the kinetic evolution of the difference spectra indicates that, within the time resolution of the technique, protonation of Glu-L212 proceeds in concomitance with electron transfer.

### 3.3. DN(L210) and DN(M17) single mutants

In the DN(L210) mutant (Fig. 5A) the difference spectrum obtained from the first scan, recorded between 4 and 29 ms after the actinic laser flash, showed contributions from $Q_A^-$ (positive peak at 1467 $cm^{-1}$, negative peak at 1670 $cm^{-1}$) but also from $Q_B^-/Q_B$ (negative band at 1640 $cm^{-1}$, positive shoulder at $\sim$1479 $cm^{-1}$). The second spectrum recorded between 79 and 104 ms after the laser flash and all spectra recorded later did not show any more bands characteristic of reduced $Q_A$ while the characteristic features of $Q_B^-$ became much clearer. In particular, a strong positive band at 1479 $cm^{-1}$ appeared, together with the positive band at 1728 $cm^{-1}$ characteristic of protonated Glu-L212. Again these $Q_B^-/Q_B$ spectra compare well with the steady-state spectrum (Fig. 5A, lowest trace, from [34]). The kinetic behavior shows that in this single mutant the electron transfer to $Q_B$ is significantly faster than in the double mutant. As the kinetics in the DN(L210) mutant was faster than the time-resolution of the rapid-scan technique, a precise kinetic analysis was

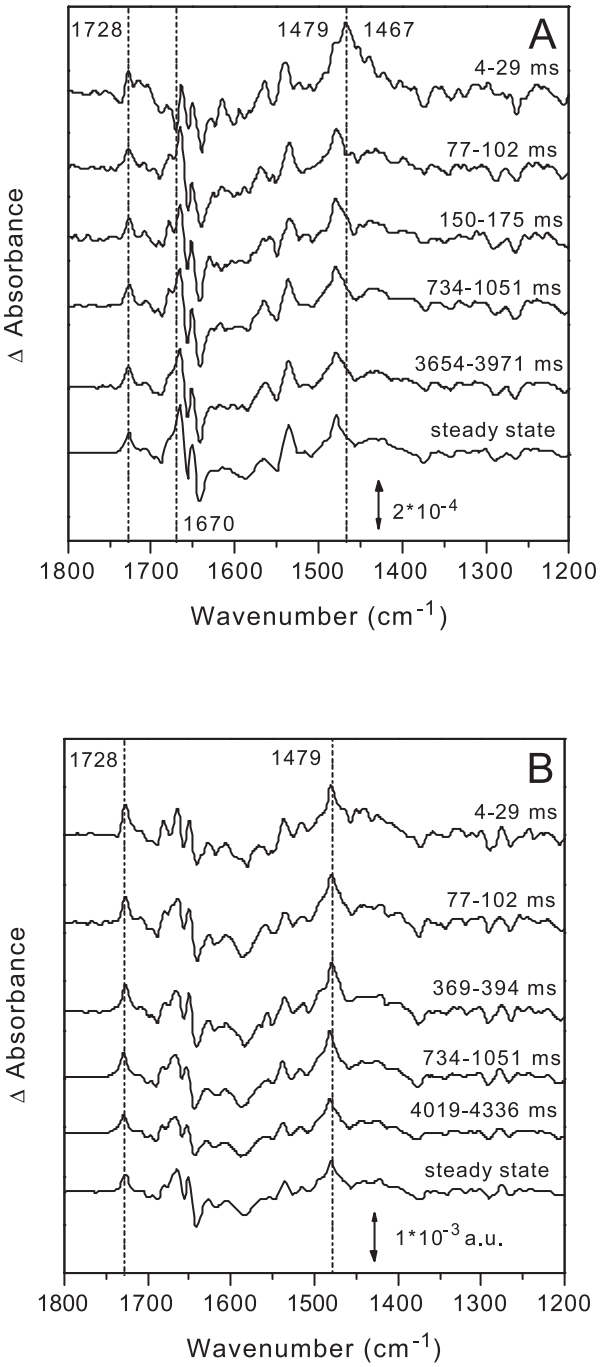


Fig. 5. Rapid-scan spectra of (A) the DN(L210) and (B) the DN(M17) single mutants at different times after a saturating laser flash. The lowest traces show the $Q_B^-/Q_B$ spectra obtained under steady-state conditions (from [34]). Note the rapid formation of $Q_B^-$ ($\tau < \sim 10$ ms) in both single mutants.

not possible. Nevertheless, the comparison between the first and the second scan clearly shows the evolution of the electron transfer reaction and its coupling with the protonation of Glu-L212.

In the DN(M17) mutant no appreciable change of the spectra with time was observed (Fig. 5B). Already the first spectrum, recorded between 4 and 29 ms after the laser flash, was characteristic of $Q_B$ reduction. No features of a $Q_A^-/Q_A$ spectrum can be discerned. This shows that in the DN(M17) mutant the $Q_A^-Q_B \rightarrow Q_AQ_B^-$ reaction is even faster than in the DN(L210) mutant and is comparable to that observed in native RCs.

## 4. Discussion

The goal of this study was the investigation of the electron transfer $Q_A^-Q_B \rightarrow Q_AQ_B^-$ and the concomitant proton uptake reaction. We used time-resolved FTIR difference spectroscopy, a technique which provides marker bands for specific redox states of the quinone electron acceptors as well as for the protonation state of amino acid side chains. Previous work based on static FTIR difference spectroscopy using isotope-labeled quinones, $^1H/^2H$ exchange, and site-directed mutant RCs has led to the assignment of several marker bands characteristic of reaction states that are stable on a time scale of tens of seconds. In this work the emphasis is on the transition between distinct reaction states. The increased information content of kinetically resolved spectroscopy can give further insight into details of the molecular scenario of the electron and proton transfer reaction in the RCs.

### 4.1. The $Q_A^-/Q_A$ difference spectrum in the double mutant

As presented in Fig. 3, the dynamic approach used in this work allowed for the first time to record a $Q_A^-/Q_A$ spectrum in presence of a functional $Q_B$, although at the expense of mutation of two amino acids involved in proton transfer to $Q_B$. Previous $Q_A^-/Q_A$ spectra [35,39,40] where always obtained on $Q_B$-depleted RCs or in presence of an inhibitor which binds to the reaction center displacing $Q_B$ from its site. It is interesting to make a comparison between the $Q_A^-/Q_A$ difference spectrum in the double mutant recorded either by the rapid-scan technique or in the static mode in presence of the inhibitor stigmatellin. This comparison is shown in Fig. 4B. Since the two spectra are well comparable, it can be argued that the presence of the inhibitor stigmatellin in the $Q_B$ site does not induce large perturbations on the $Q_A$ site. On the other hand, this comparison can be taken as further evidence that the difference spectrum on the first scan in the double mutant represents a pure $Q_A^-/Q_A$ difference spectrum.

### 4.2. Comparison of rapid-scan FTIR and transient absorption spectroscopy data

The classical method to determine the rate constant of first electron transfer from $Q_A^-$ to $Q_B$ is based on optical detection of absorption changes related to the electrochromic bandshift of BPhe which is different in the states $Q_A^-Q_B$ and $Q_AQ_B^-$ [42]. However, it has been reported that the electrochromic response is not selectively sensitive to electron transfer but may also contain contributions from relaxation events or proton uptake ([27,43] and references therein). In contrast, time-resolved FTIR difference spectroscopy provides marker bands for the different redox states of the cofactors (1467 $cm^{-1}$ (+) and 1601 (−) for $Q_A$ reduction, 1479 $cm^{-1}$ (+) and 1640 $cm^{-1}$ (−) for $Q_B$ reduction [16]), for change in the protonation state of Glu L212 (1728 $cm^{-1}$ (+) [8,27]), and for protein rearrangement (1670 $cm^{-1}$ (−) [24], 1650 $cm^{-1}$ (−) [44]). These bands are due to specific molecular vibrations and therefore represent direct and multiple probes to follow simultaneously the time course of electron transfer, proton uptake, and protein rearrangement.

In the double mutant all rapid-scan difference spectra can be well simulated by a combination of pure $Q_A^-/Q_A$ and $Q_B^-/Q_B$ spectra (Fig. 4A). This means that all bands evolve with the same kinetics, making meaningful a global fit of the spectral evolution in the 1800–1200 $cm^{-1}$ region. The global fit yielded a time constant of $\sim$40 ms for the dominant transition. According to optical kinetic measurements of the electrochromic shift of RCs in solution [13], the first electron transfer $Q_A^-Q_B \rightarrow Q_AQ_B^-$ ($k_{AB}^{(1)}$) occurs in $\sim$10 ms in the double mutant DN(L210)/DN(M17). The slightly slower kinetics observed with

rapid-scan FTIR compared to optical measurements are most probably due to the difference in temperature at which measurements were performed (281 and 294 K, respectively).

The possibility offered by FTIR difference spectroscopy to follow simultaneously the whole 1800–1200 $cm^{-1}$ spectral range allows for several other observations. First, as discussed earlier, there is no evidence for an intermediate reaction state. This points towards the absence of a transient protonation of a Glu or Asp side chain on the time scale of the measurements. Second, the results show that, within the time resolution of the technique, electron transfer to $Q_B$ and protonation of Glu-L212 are concomitant. Global proton uptake measured using pH-sensitive dyes have previously shown the very same kinetics for proton uptake as for electrochromic shift in the DN(L210)/DN(M17) double mutant [13]. It therefore appears that the kinetics of protonation of Glu-L212, of proton uptake from the cytoplasm, and of electron transfer are coupled.

In the case of the single mutants the rapid-scan measurements allow only a qualitative estimation of the reaction rates but clearly confirm the order of reaction rates for $k_{AB}^{(1)}$, i.e., DN(L210)/DN(M17) < DN(L210) < DN(M17) < native, determined by the electrochromic shift measurements [13]. In addition the results presented here clearly show that protonation of Glu-L212 in the single mutants is faster than in the double mutant. In the DN(M17) single mutant and in native RCs the first electron transfer to $Q_B$ is too fast to be resolved by the rapid-scan technique. In native RCs, this reaction has been previously studied by time-resolved step-scan FTIR [28] and by single-wavelength measurements using tunable IR laser diodes [26,27]. In these studies generally biphasic kinetics had been found at specific wavelengths corresponding to reoxidation of $Q_A^-$, reduction of $Q_B$, and protonation of Glu-L212 with a fast phase of $\sim$150 μs and a slow component of $\sim$1 ms [27]. As the simplest model Hienerwadel and coworkers proposed that the fast component reflects electron transfer and the slow component proton transfer and/or conformational changes coupled to electron transfer [26,27]. Brudler and Gerwert [28] considered this interpretation as unlikely because in their measurements the $Q_A^-$ band also showed the slow kinetic component. As an alternative explanation heterogeneity of RC conformations at the quinone binding sites was proposed [28]. Obviously this heterogeneity could be related to partial protonation of Glu-L212 in the ground state if equilibration of the protonation state of Glu-L212 is slower than electron transfer. The independence of $k_{AB}^{(1)}$ on pH and the reduced proton uptake in Glu-L212→Gln mutant RCs [31] are in agreement with this interpretation and show that protonation of Glu-L212 is a requirement for favorable electron transfer. Indeed, preliminary rapid-scan experiments on the triple mutant DN(L210)/DN(M17)/EQ(L212), where the glutamine side chain simulates protonated Glu-L212, show significantly faster kinetics of $k_{AB}^{(1)}$ than in the double mutant (not shown), similar to those in the DN(L210) mutant.

### 4.3. Kinetic model

It has been established that the proton transfer pathway connecting the cytoplasmic surface to $Q_B$ involves Asp-L210 and Asp-M17. This is most directly seen by investigating the rate of the second electron transfer to $Q_B$, for which the direct coupling of electron transfer and proton transfer is well established [1]. Upon replacement of the two residues with Asn the rate of proton-coupled electron transfer, $k_{AB}^{(2)}$, was decreased $\sim$300-fold in the double mutant DN(L210)/DN(M17) compared with native RCs [13]. In the single mutants DN(L210) and DN(M17), $k_{AB}^{(2)}$ decreased only $\leq$3-fold [12,13] indicating cooperative function of the two residues. In addition, in the presence of $Cd^{2+}$, where proton transfer has been shown to be the rate-limiting step, $k_{AB}^{(2)}$ was reduced by about one order of magnitude in the DN(L210) or DN(M17) mutant [12]. These observations show that Asp-L210 and Asp-M17 are important for efficient proton transfer to the $Q_B$ site. Replacement of both these residues by non-protonatable groups creates a barrier for proton transfer from the cytoplasm towards the $Q_B$ binding site, also apparent in the strongly reduced rate of proton uptake [13]. The double mutation thereby affects mainly the kinetics ($k_{H+}$) but much less the thermodynamics of $Q_B$ function. This can be concluded from the small effect of the mutation on the stability of the $Q_B^-$ state as measured by the kinetics of charge recombination, $k_{BD}$ [13].

In the double mutant, after formation of $Q_A^-$ the system is probably under stress as the normally occurring proton flow into the $Q_B$ site (to Glu-L212), necessary for favorable electron transfer, is kinetically hindered. The question arises if under these conditions it is possible to detect an intermediate state, which could correspond to a partly relaxed state with some internal proton rearrangement. The present results give no indications for a distinct intermediate state in all investigated samples. In the double mutant, proton uptake has been shown to be slow [13]. A unique information available from the present kinetic FTIR data is that protonation of Glu-L212 is also slow.[1] This means that in the double mutant there is no fast internal proton donor to Glu-L212 but that rather protonation of Glu-L212 (and stabilization of the state $Q_B^-$) relies on proton supply from the outside. Obviously for the first reduction of $Q_B$ a residue on position L212 with an uncharged side chain would be preferable. However, it should be kept in mind that the protonatable residue Glu-L212 has an important role, which is to provide rapidly a proton to the doubly reduced $Q_BH^-$ to form the quinol species which can leave the $Q_B$ binding site.

## Acknowledgements

This work was supported by grants to M.L.P. (National Institutes of Health, NIH GM 41637) and to A.M. (Fondazione 'A. Gini', Padova).

## References

[1] M.Y. Okamura, M.L. Paddock, M.S. Graige, G. Feher, Biochim. Biophys. Acta 1458 (2000) 148–163.
[2] J.P. Allen, G. Feher, T.O. Yeates, H. Komiya, D.C. Rees, Proc. Natl. Acad. Sci. USA 85 (1988) 8487–8491.
[3] U. Ermler, G. Fritsch, S.K. Buchanan, H. Michel, Structure 2 (1994) 925–936.
[4] O. El-Kabbani, C.-H. Chang, D. Tiede, J. Norris, M. Schiffer, Biochemistry 30 (1991) 5361–5369.
[5] P. Sebban, P. Maroti, D.K. Hanson, Biochimie 77 (1995) 677–694.
[6] E. Takahashi, P. Maroti, C.A. Wraight, in: E. Diemann, W. Junge, A. Muller, H. Ratajczak (Eds.), Electron and Proton Transfer in Chemistry and Biology, Elsevier, Amsterdam, 1991, pp. 219–236.
[7] P. Maroti, Photosynth. Res. 37 (1993) 1–17.
[8] E. Nabedryk, J. Breton, R. Hienerwadel, C. Fogel, W. Mäntele, M.L. Paddock, M.Y. Okamura, Biochemistry 34 (1995) 14722–14732.
[9] P. Brzezinski, M.Y. Okamura, G. Feher, Biochim. Biophys. Acta 1321 (1997) 149–156.
[10] E.G. Alexov, M.R. Gunner, Biochemistry 38 (1999) 8253–8270.
[11] B. Rabenstein, G.M. Ullmann, E.-W. Knapp, Biochemistry 39 (2000) 10487–10496.
[12] M.L. Paddock, G. Feher, M.Y. Okamura, Proc. Natl. Acad. Sci. USA 97 (2000) 1548–1553.
[13] M.L. Paddock, P. Ädelroth, C. Chang, E.C. Abresch, G. Feher, M.Y. Okamura, Biochemistry 40 (2001) 6893–6902.
[14] M.S. Graige, G. Feher, M.Y. Okamura, Proc. Natl. Acad. Sci. USA 95 (1998) 11679–11684.
[15] M.H.B. Stowell, T.M. McPhillips, D.C. Rees, S.M. Soltis, E. Abresch, G. Feher, Science 276 (1997) 812–816.
[16] J. Breton, E. Nabedryk, Biochim. Biophys. Acta 1275 (1996) 84–90.
[17] W. Mäntele in: R.E. Blankenship, M.P.T. Madigan, C.E. Bauer (Eds.), Advances in Photosynthesis: Anoxygenic Photosynthetic Bacteria, Kluwer Academic Publishers, Dordrecht, 1995, pp. 627–647.
[18] E. Nabedryk, in: H.H. Mantsch, D. Chapman (Eds.), Infrared Spectroscopy of Biomolecules, Wiley-Liss, New York, 1996.
[19] M.S. Braiman, P.L. Ahl, K.J. Rothschild, Proc. Natl. Acad. Sci. USA 84 (1987) 5221–5225.
[20] W. Mäntele, in: J. Amesz, A.J. Hoff (Eds.), Biophysical Techniques in Photosynthesis, Kluwer Academic Publishers, Dordrecht, 1996, pp. 137–160.
[21] K. Gerwert, in: H.-U. Gremlich, B. Yan (Eds.), Infrared and Raman Spectroscopy of Biological Materials, Marcel Dekker, New York, 2000, pp. 193–230.
[22] F. Siebert, in: H.H. Mantsch, D. Chapman (Eds.), Infrared Spectroscopy of Biological molecules, Wiley-Liss, New York, 1996, pp. 83–106.
[23] W. Uhmann, A. Becker, C. Taran, F. Siebert, Appl. Spectrosc. 45 (1991) 390–397.
[24] D.L. Thibodeau, E. Nabedryk, T. Hienerwadel, F. Lenz, W. Mäntele, J. Breton, Biochim. Biophys. Acta 1020 (1990) 243–259.
[25] D. Kleinfeld, M.Y. Okamura, G. Feher, Biochim. Biophys. Acta 766 (1984) 126–140.
[26] R. Hienerwadel, D.L. Thibodeau, F. Lenz, E. Nabedryk, J.

[1] The amplitude of the proton uptake by Glu-L212 is, however, increased in the single and double mutants compared to native RCs, as is evident from the larger intensity of the 1728 $cm^{-1}$ band in the steady-state spectra of the mutant RCs. This implies that the extent of ionization of Glu-L212 in the $Q_B$ ground state is increased in the mutants compared to native RCs [34].

Breton, W. Kreutz, W. Mäntele, Biochemistry 31 (1992) 5799–5808.
[27] R. Hienerwadel, S. Grzybek, C. Fogel, W. Kreutz, M.Y. Okamura, M.L. Paddock, J. Breton, E. Nabedryk, W. Mäntele, Biochemistry 34 (1995) 2832–2843.
[28] R. Brudler, K. Gerwert, Photosynth. Res. 55 (1998) 261–266.
[29] P. Ädelroth, M.L. Paddock, L.B. Sagle, G. Feher, M.Y. Okamura, Proc. Natl. Acad. Sci. USA 97 (2000) 13086–13091.
[30] A. Mezzetti, E. Nabedryk, J. Breton, M.Y. Okamura, M.L. Paddock, W. Leibl, Biophys. J. 80 (2001) 428a.
[31] M.L. Paddock, S.H. Rongey, G. Feher, M.Y. Okamura, Proc. Natl. Acad. Sci. USA 86 (1989) 6602–6606.
[32] R.A. Isaacson, F. Lendzian, E.C. Abresch, W. Lubitz, G. Feher, Biophys. J. 69 (1995) 311–322.
[33] J.O. Lephardt, G. Vilcins, Appl. Spectrosc. 29 (1975) 221–225.
[34] E. Nabedryk, J. Breton, M.Y. Okamura, M.L. Paddock, Biochemistry 40 (2001) 13826–13832.
[35] J. Breton, D.L. Thibodeau, C. Berthomieu, W. Mäntele, A. Verméglio, E. Nabedryk, FEBS Lett. 278 (1991) 257–260.
[36] J. Breton, C. Berthomieu, D.L. Thibodeau, E. Nabedryk, FEBS Lett. 288 (1991) 109–113.
[37] J. Breton, C. Boullais, G. Berger, C. Mioskowski, E. Nabedryk, Biochemistry 34 (1995) 11606–11616.
[38] R. Brudler, H.J.M. de Groot, W.B.S. van Liemt, P. Gast, A.J. Hoff, J. Lugtenburg, K. Gerwert, FEBS Lett. 370 (1995) 88–92.
[39] J. Breton, C. Boullais, J.-R. Burie, E. Nabedryk, C. Mioskowski, Biochemistry 33 (1994) 14378–14386.
[40] R. Brudler, H.J.M. de Groot, W.B.S. van Liemt, W.F. Steggerda, R. Esmeijer, P. Gast, A.J. Hoff, J. Lugtenburg, K. Gerwert, EMBO J. 13 (1994) 5523–5530.
[41] J. Breton, E. Nabedryk, J.P. Allen, J.C. Williams, Biochemistry 36 (1997) 4515–4525.
[42] A. Verméglio, R.K. Clayton, Biochim. Biophys. Acta 461 (1977) 159–165.
[43] D.M. Tiede, L. Utschig, D.K. Hanson, D.M. Gallo, Photosynth. Res. 55 (1998) 267–273.
[44] E. Nabedryk, K.A. Bagley, D.L. Thibodeau, M. Bauscher, W. Mäntele, J. Breton, FEBS Lett. 266 (1990) 59–62.